IAES International Journal of Artificial Intelligence (IJ-AI)
Vol. 15, No. 3, June 2026, pp. 2698∼2708
ISSN: 2252-8938, DOI: 10.11591/ijai.v15.i3.pp2698-2708 ❒ 2698

Parkinsonian gait classification in older adults using time–frequency spectrograms and 2D convolutional neural network

Kazi Ashikur Rahman, Ezreen Farina Shair, Nur Zawani Saharuddin, Muhammad Hazwan Adlin Jumaris
Rehabilitation and Assistive Technology Research Group, Faculty of Electrical Technology and Engineering,
Universiti Teknikal Malaysia Melaka, Melaka, Malaysia

Article Info

Article history:

Received Dec 29, 2024
Revised Mar 17, 2026
Accepted Apr 22, 2026

Keywords:

2D convolutional neural network
Continuous wavelet transform
Convolutional neural networks
Gait disorders
Neurodegenerative diseases
Older adults
Parkinson's disease

ABSTRACT

Gait disorders in adults aged 50 years and above are a common concern and are often linked to reduced mobility, a higher risk of falls, and a lower quality of life. This study presents a deep learning-based approach to detect gait disorders using vertical ground reaction force (vGRF) signals. The data were collected from older adults, including individuals with Parkinson's disease (PD) and healthy controls, using force-sensitive resistor sensors. The raw signals were first processed using band-pass filtering and wavelet denoising to remove noise and unwanted variations. After that, the signals were converted into time–frequency representations using the continuous wavelet transform (CWT). These representations were then used as input to a convolutional neural network (CNN) for classification. The model achieved a validation accuracy of 93.48%, with precision, recall, and F1-score all above 92% for both groups. The results show that combining CWT with CNN provides a reliable and efficient way to detect gait disorders. This approach can support clinical evaluation by offering a practical and scalable method for analyzing gait patterns in older adults.

Corresponding Author:

Ezreen Farina Shair
Rehabilitation and Assistive Technology Research Group, Faculty of Electrical Technology and Engineering
Universiti Teknikal Malaysia Melaka
Melaka, Malaysia
Email: ezreen@utem.edu.my

1. INTRODUCTION

Gait refers to the pattern of walking produced through the coordinated action of the brain, nervous system, and musculoskeletal structures [1]. Among individuals aged 50 and above, gait disorders represent a growing public health concern. These conditions are associated with an elevated risk of falls, contributing to approximately 646,000 fatalities annually and incurring substantial healthcare costs, accounting for 0.85% to 1.5% of global expenditure [2]–[4]. As the prevalence of gait disorders continues to rise within this demographic, the need for advanced and accurate diagnostic tools becomes increasingly urgent [5], [6].

Neurodegenerative diseases (NDDs), including Parkinson's disease (PD) and Huntington's disease (HD), are among the primary conditions associated with abnormal gait patterns. In the case of PD, walking impairments commonly present as shortened stride length, reduced postural control, and shuffling steps, all of which lead to a marked decline in functional mobility and independence [7], [8]. Identifying these subtle gait alterations, especially in their early stages, is challenging with conventional diagnostic methods. Emerging technologies like deep learning provide promising avenues for improving the analysis and classification of gait patterns with enhanced precision [9]–[11].

Convolutional neural networks (CNNs), a key category within deep learning, have demonstrated strong performance in both image and signal classification applications, making them highly suitable for gait analysis. In contrast to conventional approaches, CNNs are capable of learning discriminative features directly from raw input data, eliminating the reliance on manual feature extraction and overcoming several limitations of traditional methods. In this study, CNNs are integrated with continuous wavelet transform (CWT) for feature extraction to enable effective classification of gait patterns associated with PD in older adults. Recent research underscores the versatility of CNNs in analyzing gait data. For instance, Shalin *et al.* [12] leveraged plantar pressure data with CNN models to predict freezing of gait in PD patients, achieving commendable sensitivity and specificity. However, their study focused on specific gait abnormalities, limiting its generalizability to broader disorders. Kumari and Ramachandran [13] demonstrated the efficacy of deep CNNs in analyzing speech-related features, achieving high classification accuracy, but their approach lacked integration with gait-specific data. Similarly, Rahman *et al.* [14] utilized CWT and CNNs to analyze vertical ground reaction force (vGRF) data for gait classification, achieving a validation accuracy of 95.06%. However, their reliance on single-modal data limited the broader applicability of their findings.

Efforts to enhance performance and applicability have included multimodal and explainable architectures. Ma *et al.* [15] developed an explainable CNN framework for early PD diagnosis, achieving over 98% accuracy through effective feature selection and data balancing, though its explainability was constrained to selected features. Shao *et al.* [16] integrated skeleton and silhouette data in a multimodal framework for depression detection, demonstrating flexibility for complex datasets but focusing on depression rather than gait disorders. Sánchez *et al.* [17] employed a two-stage neural network for gait analysis using smartphone sensors, achieving reliable early PD detection, though sensor dependency presented challenges for real-world applications. Peimankar *et al.* [18] utilized particle swarm optimization (PSO) to enhance accelerometer data classification with CNNs, achieving 93.32% accuracy despite challenges with sensor placement. Other notable methods include quantitative susceptibility mapping for early-stage PD diagnosis [19], gait feature classification using inertial measurement units (IMU) data [20], and neuroimaging-based cognitive phenotype identification for PD [21].

Despite these advancements, critical gaps persist. Most studies rely on general age datasets or single-modal data, which fail to capture the nuanced variations in gait patterns unique to older adults with neurodegenerative disorders. For example, while vGRF data combined with CNNs has demonstrated promising results [14], the absence of multimodal data integration limits robustness. Moreover, approaches using smartphone sensors [17] or accelerometers [18] often encounter practical limitations due to device dependency and inconsistent sensor placements. Additionally, explainable CNN frameworks [15] and multimodal architectures [16] often emphasize accuracy but are not specifically tailored to gait-specific disorders like HD, leaving this area underexplored. To overcome these limitations, this study makes use of vGRF signals and applies the CWT for detailed feature representation, followed by CNN–based classification. Unlike many earlier studies that rely on mixed-age datasets, the present work concentrates specifically on older adults, who are most vulnerable to gait-related impairments. The proposed approach combines scalable deep learning techniques to support the early identification and assessment of gait abnormalities, with particular relevance to neurodegenerative conditions such as PD.

2. METHOD

The methodology illustrated in Figure 1 was followed to develop the deep learning model for PD gait disorder detection. This study involved three key processes: data collection, preprocessing, and deep learning model development. Gait data was collected from healthy individuals and those diagnosed with PD. The raw data underwent preprocessing steps such as noise reduction using a band-pass filter, window selection, and transformation into time-frequency spectrograms using CWT. Data augmentation techniques were then applied to increase variability and robustness. Finally, CNN was trained to classify gait patterns associated with PD.

2.1. Gait data source and characteristics

This study makes use [11]. The dataset contains vGRF measurements acquired through force-sensitive resistor sensors positioned beneath the feet inside participants' footwear. During data collection, participants were asked to walk along a 77-meter indoor corridor for a duration of five minutes at a self-selected, comfortable walking speed, while gait force signals were recorded continuously.

The dataset includes recordings from a total of 64 participants aged 50 years and above, consisting of 15 individuals diagnosed with PD and 16 age-matched healthy control subjects (CO). Several gait-related parameters were captured, including stance phase, swing phase, double support interval, and stride characteristics, for both left and right feet. To ensure uniformity in analysis and to limit computational demands, only right-foot vGRF signals were considered in this work. Across the five-minute walking trials, each participant contributed an average of approximately 277 gait cycles. A summary of the participants' demographic and clinical information is provided in Table 1.

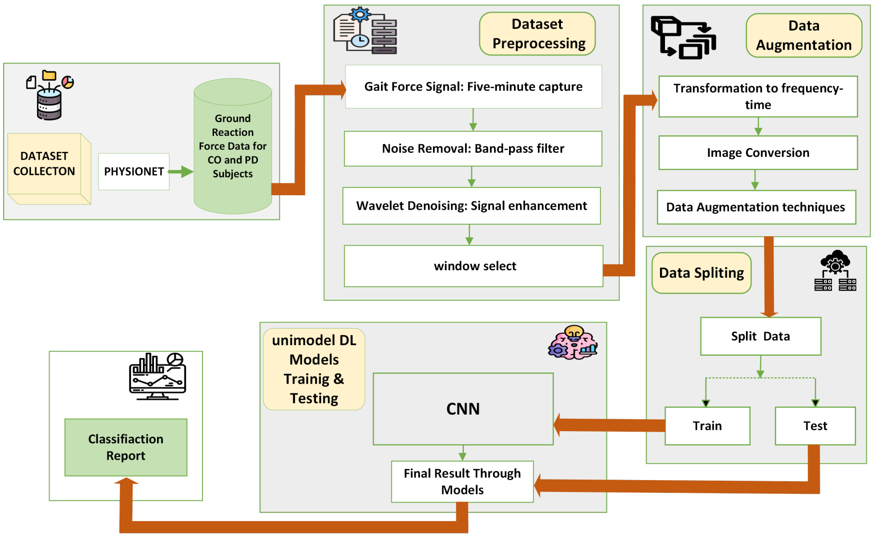

Figure 1. Diagram of the proposed method for PD gait classification

Table 1. Participant information for PD gait analysis

Parameter	Healthy controls (CO)	PD patients
Age (Years)	62.6 ± 8.63	66.5 ± 9.06
Height (m)	1.84 ± 0.10	1.99 ± 0.12
Weight (kg)	74.6 ± 13.02	87.38 ± 13.68
Gait speed (m/s)	1.29 ± 0.21	1.34 ± 0.27

2.2. Data preprocessing

Prior to model training, the vGRF signals underwent a series of preprocessing steps to improve signal quality and suitability for deep learning analysis [22]. Initially, noise components present in the raw recordings were attenuated using a digital band-pass filtering approach, which can be expressed as in (1).

$$s_f(t) = (s * h)(t) \tag{1}$$

In this formulation, $x(t)$ $x(t)$ represents the original input signal, $h(t)$ represents the impulse response of the filter, and it $y(t)$ corresponds to the filtered output signal [23]. To further suppress residual noise and enhance signal clarity, wavelet-based denoising was applied. This process involves decomposing the filtered signal into wavelet coefficients, applying thresholding, and reconstructing the signal as described by (2).

$$z(t) = \mathcal{W}^{-1}\left(\Theta(\mathcal{W}(y(t)))\right) \tag{2}$$

Following denoising, the refined vGRF signals were divided into non-overlapping segments of 10 seconds to ensure adequate time–frequency representation. The CWT was subsequently employed to convert each segment into a time–frequency spectrogram, allowing the CNN to capture both temporal dynamics and frequency-related characteristics of gait signals [24].

2.3. Data augmentation

To improve the robustness of the proposed model and minimize the risk of overfitting, multiple augmentation techniques were applied to the gait data after transforming it into the frequency-time domain. These augmentations simulate variations such as orientation, lighting, and focus conditions. This enhanced the variability and realism of the training dataset, allowing the CNN to learn more robust features.

Horizontal flipping was implemented, where the transformation $f(x, y) \rightarrow f(-x, y)$ inverted the image along the vertical axis. Additionally, random rotations were applied within a range of -10 to 10 degrees, following the transformation matrix shown in (3).

$$\begin{pmatrix} \cos\theta & -\sin\theta \\ \sin\theta & \cos\theta \end{pmatrix} \tag{3}$$

To simulate shifts in spatial positioning, random translations were performed along the x and y axes, described mathematically as in (4).

$$(x, y) \rightarrow (x + \Delta x, y + \Delta y) \tag{4}$$

Brightness and contrast levels were adjusted to replicate various lighting conditions, using (5).

$$I' = \alpha I + \beta \tag{5}$$

Scaling was used to create size variations within the dataset, as shown in (6).

$$(x, y) \rightarrow (sx, sy) \tag{6}$$

To mimic differences in focus and sharpness, Gaussian blur was applied, defined by (7).

$$G(x, y) = \frac{1}{2\pi\sigma^2} \exp\left(-\frac{x^2 + y^2}{2\sigma^2}\right) \tag{7}$$

These transformations generated new variations of the input data by altering its size, position, brightness, and focus levels, thus enhancing the dataset's robustness. By introducing such variability, the CNN model was better equipped to classify gait patterns under diverse conditions, ultimately reducing the risk of overfitting.

2.4. Classification model

The classification framework is based on a CNN designed to distinguish gait patterns between PD and CO groups using time–frequency representations derived from the CWT. As illustrated in Figure 2, the network is composed of five convolutional stages that progressively learn discriminative features from the input spectrograms. Each convolutional layer is followed by a rectified linear unit (ReLU) activation function and a max-pooling step, which reduce the feature dimensions while improving computational efficiency. The resulting feature representations are then forwarded to fully connected layers, where the model computes the probability distribution for PD and CO classes through a Softmax output layer.

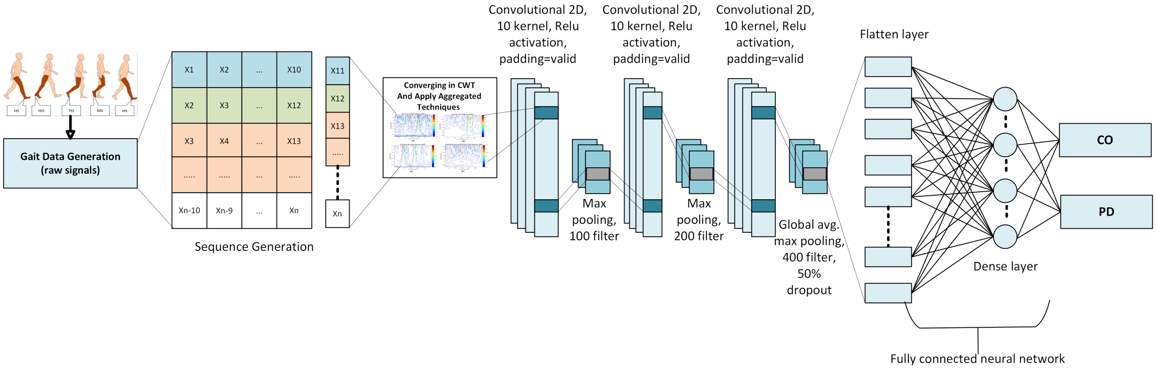

Figure 2. CNN architecture used for classifying PD and CO gait patterns from spectrogram images

2.4.1. Convolutional neural network architecture

The input layer processes images of size 224×224×3. The convolutional layers utilize filters of increasing depth (32, 64, 128, 256, and 512), each followed by ReLU activation and 2×2 max-pooling to enable hierarchical feature learning. The fully connected section includes a dense layer with 512 neurons, followed by another with 256 neurons, both using ReLU activation. The final output layer consists of two neurons with a Softmax activation function to produce classification probabilities for PD and CO. This design efficiently combines convolutional layers for feature extraction and dense layers for classification, ensuring robust performance in distinguishing PD from CO.

2.5. Mathematical formulation

The CNN model processes input images through multiple layers, where each convolutional layer l applies filters W_l and biases b_l to produce feature maps, as expressed in (8).

$$O_l = f(W_l * I_{l-1} + b_l) \tag{8}$$

Here, * represents convolution, and $f(x) = \max(0, x)$ is the ReLU activation function. Pooling layers perform spatial downsampling to reduce dimensionality while keeping important feature information as in (9).

$$P_l = \text{pool}(O_l) \tag{9}$$

Finally, the fully connected layers combine features and use the softmax function to generate class probabilities, as shown in (10).

$$Y_k = \frac{\exp(z_k)}{\sum_{j=1}^{K} \exp(z_j)} \tag{10}$$

The model is trained by minimizing the categorical cross-entropy loss, defined in (11).

$$L = -\sum_{i=1}^{N} \sum_{k=1}^{K} y_{i,k} \log(\hat{y}_{i,k}) \tag{11}$$

Here, $y_{i,k}$ indicates the true class label (1 if correct, else 0), and $\hat{y}_{i,k}$ is the predicted probability for class k.

2.6. Model performance assessment

The effectiveness of the proposed model in distinguishing gait patterns between PD and CO groups was evaluated using standard classification metrics derived from the confusion matrix. This matrix summarizes prediction outcomes in terms of correctly and incorrectly classified samples. Specificity, defined in (12), was used to measure the model's capability to correctly identify control cases. Sensitivity, also referred to as recall and given in (13), represents the proportion of PD cases that were accurately detected. The overall classification accuracy, calculated using (14), measures the fraction of correctly predicted instances with respect to the total number of observations. Precision, expressed in (15), indicates the reliability of positive predictions, while the F1-score in (16) provides a balanced measure by jointly considering precision and sensitivity. Collectively, these metrics offer a comprehensive assessment of the model's performance in classifying gait patterns based on vGRF data.

$$\text{Specificity} = \frac{\sum_{k=1}^{m} N_{c,k}}{\sum_{k=1}^{m} (N_{c,k} + P_{e,k})} \tag{12}$$

$$\text{Sensitivity} = \frac{\sum_{k=1}^{m} P_{c,k}}{\sum_{k=1}^{m} (P_{c,k} + N_{e,k})} \tag{13}$$

$$\text{Accuracy} = \frac{\sum_{k=1}^{m} (P_{c,k} + N_{c,k})}{\sum_{k=1}^{m} (P_{c,k} + N_{c,k} + P_{e,k} + N_{e,k})} \tag{14}$$

$$\text{Precision} = \frac{TP}{TP + FP} \tag{15}$$

$$\text{F1-score} = \frac{2 \times (\text{Precision} \times \text{Sensitivity})}{\text{Precision} + \text{Sensitivity}} \tag{16}$$

3. RESULTS AND DISCUSSION

In this research, MATLAB version 2022b served as the primary tool for data reprocessing, data augmentation, and training the deep learning model. Its integrated support for image processing and deep learning toolboxes facilitated the transformation of vGRF data into CWT-based spectrograms and the training of the CNN model. MATLAB also supports visualization and evaluation of training performance metrics, ensuring reproducibility and clarity.

3.1. Statistical analysis

Table 2 highlights key differences in the time and frequency domain gait signals for the control (CO) and PD groups. In the time domain, CO signals exhibit stable amplitude and stride intervals, indicating consistent gait patterns. Conversely, PD signals reveal irregularities, such as fluctuating amplitudes and interrupted intervals, which are symptomatic of motor impairments like bradykinesia and freezing of gait. Frequency-domain analysis, derived using CWT, further emphasizes these differences. CO signals show compact energy distributions, reflecting rhythmic gait, while PD signals display dispersed and fragmented patterns, indicating variability and reduced motor control.

Table 2. Time and frequency-domain representations of gait signals for CO and PD groups

CO		PD	
Time domain gait signal	Frequency domain gait signal	Time domain gait signal	Frequency domain gait signal
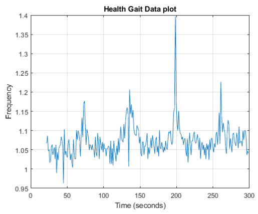	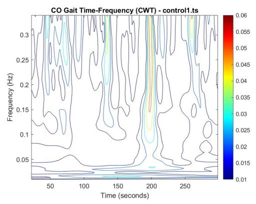	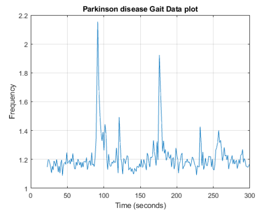	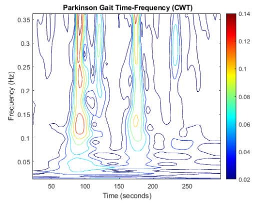
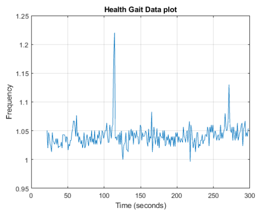	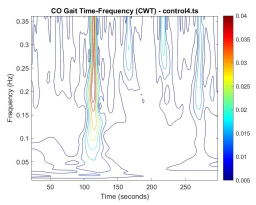	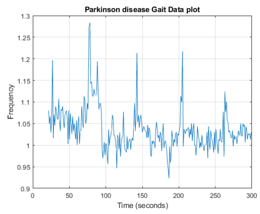	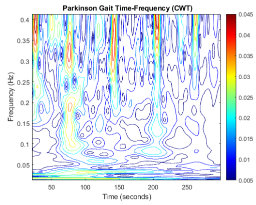
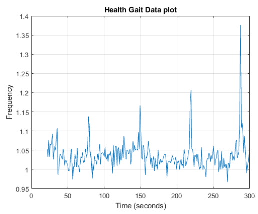	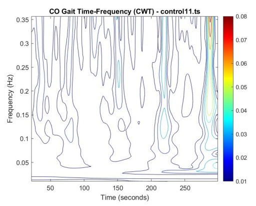	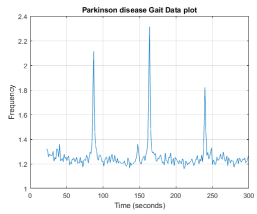	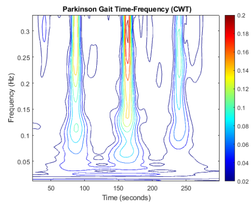

Figure 3 compares statistical gait features between CO and PD groups using box plots. The mean gait speed for PD patients is significantly lower, highlighting their reduced mobility. PD patients also exhibit greater variability, as indicated by wider interquartile ranges (IQRs) for standard deviation and variance, compared to the CO group. Additionally, root mean square (RMS) and instantaneous RMS values are more dispersed for PD, reflecting unstable gait patterns. These statistical insights demonstrate the distinct gait characteristics of PD, which are critical inputs for training deep learning models. Integrating these features into CNN frameworks enables accurate classification of gait disorders, facilitating early diagnosis and targeted intervention for NDDs.

3.2. Convolutional neural network model training progress

Figure 4 illustrates the progression of the CNN model during training, achieving a final validation accuracy of 93.48% after 90 iterations over 30 epochs. The initial learning rate was set to $\eta = 0.001$, ensuring a stable convergence of the optimization process. The training objective was to minimize the categorical cross-entropy loss function, as defined in (11), where $N = 90$ represents the total number of training iterations and $K = 2$ denotes the binary classification of the two classes: CO and PD. In this context, $y_{i,k}$ corresponds to the correct class indicator, while $\hat{y}_{i,k}$ reflects the probability output generated by the model for class k.

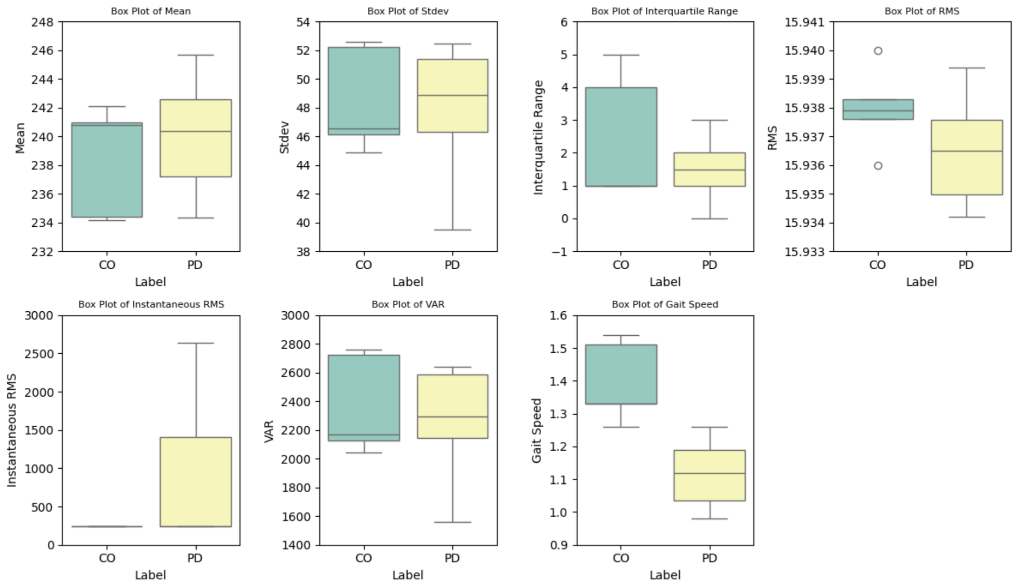

Figure 3. Comparison of gait features between PD and CO groups using box plots

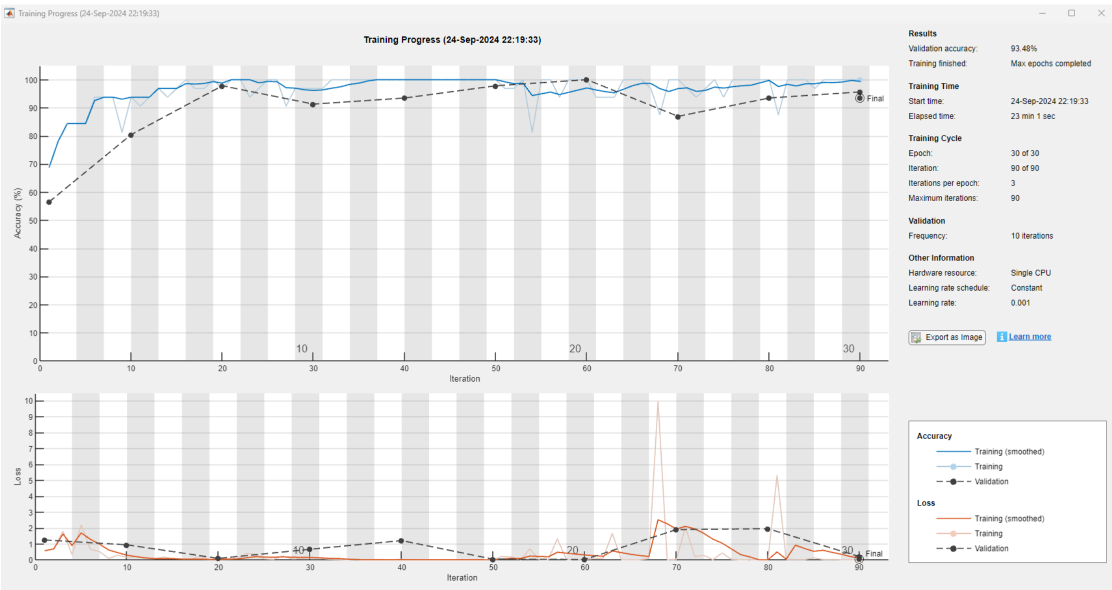

Figure 4. Training progress of the CNN model for PD vs. CO classification

3.3. Convolutional neural network classification analysis using the confusion matrix

The CNN confusion matrix of the validation results provides a detailed overview of the CNN model's classification performance for both the control (CO) and PD classes. The results summarise the number of correctly and incorrectly classified samples for each class, offering insight into the model's classification behaviour and class-wise balance. For the CO class, out of 19 samples, 17 were correctly classified, resulting in an accuracy of 89.5%, while 2 samples were misclassified as PD. For the PD class, 26 out of 27 samples were correctly classified, achieving a higher accuracy of 96.3%, with only 1 sample misclassified as CO. These results indicate strong classification performance for both classes, with a slightly higher classification rate for the PD group. The relatively low number of misclassified samples demonstrates the capability of the CNN model to effectively distinguish between CO and PD gait patterns. Overall, the high classification accuracy and low misclassification rates highlight the reliability and robustness of the CNN model in analyzing gait patterns associated with neurodegenerative disorders.

3.4. Classification results

The proposed CNN model achieved a validation accuracy of 93.48% for the binary classification task involving CO and PD. Precision was strong at 92.88%, while recall (sensitivity) reached 93.65%. The F1-score, which balances precision and recall, was 93.2%, reflecting the model's robustness across these metrics. Table 3 presents the detailed classification results, including precision, sensitivity, specificity, and F1-scores for both CO and PD classes. Specificity values were consistent, with CO achieving 92.86% and PD slightly higher at 94.44%. The F1-scores of 91.89% for CO and 94.56% for PD highlight the model's capability to accurately differentiate between the two classes, balancing false positives and false negatives. These results underscore the utility of leveraging CWT for feature extraction, enabling the CNN to accurately distinguish between the two gait classes.

Table 3. Performance metrics for the CNN model

Metric	Control (CO)	PD
Validation accuracy (%)	93.48	
Precision (%)	89.47	96.30
Sensitivity (%)	94.44	92.86
Specificity (%)	92.86	94.44
F1-score (%)	91.89	94.56

3.5. Discussion and comparison

This research emphasizes the gait disorder classification in older adults, a group profoundly impacted by neurodegenerative conditions such as PD. The methodology uses vGRF data processed through CWT and leverages CNN for classification. Achieving a validation accuracy of 93.48%, the proposed approach demonstrates strong precision, sensitivity, and F1 scores, positioning it as competitive with similar studies, such as Rahman *et al.* [14] (95.06%) and Yan *et al.* [25] (97.42%). Unlike these studies, which included broader populations or simpler datasets, the focus here on older adults enhances the clinical relevance and utility of the model. While Ma *et al.* [15] achieved a higher accuracy of 98% using IMU-derived features, our approach is less reliant on specialized sensors, making it more accessible for widespread clinical use. A detailed comparison of classification results from various recent deep learning approaches is presented in Table 4.

Table 4. Classification results of CO and PD using various deep learning methods

Study	Signal	Methodology	Validation accuracy (%)	Precision (%)	Sensitivity (%)	Specificity (%)	F1-score (%)
Shalin *et al.* [12]	Plantar pressure data	Statistical features + CNN	93.33	90.21	91.12	89.00	90.67
Rahman *et al.* [14]	VGRF	CWT + ResNet-50	95.06	92.85	94.00	93.10	93.42
Sánchez *et al.* [17]	Smartphone sensor data	Two-stage neural network + CNN	91.68	88.12	89.45	87.32	88.77
Ma *et al.* [15]	IMU-derived features	Explainable CNN framework	98.00	95.50	96.30	94.80	95.90
Peimankar *et al.* [18]	Accelerometer data	PSO + CNN	93.32	91.10	92.20	90.15	91.64
Yan *et al.* [25]	VGRF	Time-frequency spectrogram + Deep CNN	97.42	94.80	95.60	94.50	95.20
Erdas *et al.* [19]	VGRF	Recurrence plot + CNN	98.93	96.00	96.85	95.90	96.42
Lin *et al.* [20]	VGRF	Raw VGRF data + SVM	81.00	78.90	79.80	78.00	79.34
This study	VGRF	Time-frequency spectrogram + CNN	93.48	92.89	93.65	92.86	93.22

The table summarizes accuracy, precision, sensitivity, specificity, and F1-scores across studies using different signal types and model architectures for PD and control group classification. Despite the robust results, this study has limitations, such as the exclusive reliance on vGRF data and the focus on binary classification. Future work should explore multimodal datasets, integrating IMU, electromyography (EMG), and neuroimaging data, to improve model performance and applicability to other HD and ALS. Additionally, incorporating explainability techniques into the CNN framework could foster clinical adoption and provide better insights into gait abnormalities. Overall, this study demonstrates the potential of CWT and CNN to classify gait patterns in older adults, offering a scalable and effective tool for early diagnosis and intervention.

4. CONCLUSION

This study demonstrates the effectiveness of utilizing vGRF data, processed through CWT, in combination with a CNN for classifying gait patterns in older adults with PD. The proposed method achieved a validation accuracy of 93.48%, with high precision, sensitivity, and F1 scores, showcasing its robustness in detecting subtle gait abnormalities. These findings highlight the potential of integrating CWT and CNN for developing scalable diagnostic tools for early intervention in neurodegenerative disorders. Future work will focus on incorporating multimodal datasets and explainability techniques to enhance model performance and clinical applicability.

ACKNOWLEDGMENTS

The authors acknowledge the financial support received from Universiti Teknikal Malaysia Melaka (UTeM) and Ajman University, UAE. Appreciation is also extended to UTeM for providing support through the Kesidang Scholarship. The authors would like to thank the research team members and collaborators for their support and contributions to the completion of this work.

FUNDING INFORMATION

This study was supported by the International Matching Grant collaboration between Universiti Teknikal Malaysia Melaka (UTeM) and Ajman University under Grant No: ANTARABANGSA(URMG)-AJMAN/2024/FTKE/A0067.

AUTHOR CONTRIBUTIONS STATEMENT

This journal uses the Roles Taxonomy (CRediT) to recognize individual author contributions, reduce authorship disputes, and facilitate collaboration.

Name of Author	**C**	**M**	**So**	**Va**	**Fo**	**I**	**R**	**D**	**O**	**E**	**Vi**	**Su**	**P**	**Fu**
Kazi Ashikur Rahman	✓	✓	✓	✓	✓	✓		✓	✓	✓			✓	
Ezreen Farina Shair	✓	✓		✓	✓	✓	✓	✓	✓	✓	✓	✓		✓
Nur Zawani Saharuddin		✓	✓		✓					✓	✓		✓	
Muhammad Hazwan Adlin Jumaris		✓	✓							✓				

C : **C**onceptualization	I : **I**nvestigation	Vi : **Vi**sualization
M : **M**ethodology	R : **R**esources	Su : **Su**pervision
So : **So**ftware	D : **D**ata Curation	P : **P**roject Administration
Va : **Va**lidation	O : Writing - **O**riginal Draft	Fu : **Fu**nding Acquisition
Fo : **Fo**rmal Analysis	E : Writing - Review & **E**diting	

CONFLICT OF INTEREST STATEMENT

Authors state no conflict of interest.

DATA AVAILABILITY

This study uses the gait in NDDs dataset introduced by Hausdorff *et al.* [8].

REFERENCES

[1] M. M. Lusardi *et al.*, "Determining risk of falls in community dwelling older adults: a systematic review and meta-analysis using posttest probability," *Journal of Geriatric Physical Therapy*, vol. 40, no. 1, pp. 1–36, 2017, doi: 10.1519/JPT.0000000000000099.

[2] S. Raghu, M. Raghu, A. P. Marla, S. S. Kotian, and N. Kumari, "Fall-related injuries and their prevention strategies of in-patient population in tertiary health care setup," *QAI Journal for Healthcare Quality and Patient Safety*, vol. 3, no. 1, pp. 1–7, Jan. 2022, doi: 10.4103/QAIJ.QAIJ_8_22.

[3] R. Norton *et al.*, "Nontransport unintentional injuries," in *Injury Prevention and Environmental Health*, 3rd ed., Washington, United States: The International Bank for Reconstruction and Development / The World Bank, 2017.

[4] H. Jia, E. I. Lubetkin, K. DeMichele, D. S. Stark, M. M. Zack, and W. W. Thompson, "Prevalence, risk factors, and burden of disease for falls and balance or walking problems among older adults in the U.S.," *Preventive Medicine*, vol. 126, Sep. 2019, doi: 10.1016/j.ypmed.2019.05.025.

[5] A. Ashari, T. A. Hamid, M. R. Hussain, and K. D. Hill, "Effectiveness of individualized home-based exercise on turning and balance performance among adults older than 50 yrs: a randomized controlled trial," *American Journal of Physical Medicine & Rehabilitation*, vol. 95, no. 5, pp. 355–365, May 2016, doi: 10.1097/PHM.0000000000000388.

[6] K. A. Rahman, N. H. Ali, and A. S. Muda, "A narrative review on collateral circulation classification for ischemic stroke," *Results in Engineering*, vol. 28, Dec. 2025, doi: 10.1016/j.rineng.2025.107583.

[7] J. I. Hoff, A. A. V. D. Plas, E. A. H. Wagemans, and J. J. V. Hilten, "Accelerometric assessment of levodopa-induced dyskinesias in Parkinson's disease," *Movement Disorders*, vol. 16, no. 1, pp. 58–61, Jan. 2001, doi: 10.1002/1531-8257(200101)16:1<58::aid-mds1018>3.0.co;2-9.

[8] J. M. Hausdorff, A. Lertratanakul, M. E. Cudkowicz, A. L. Peterson, D. Kaliton, and A. L. Goldberger, "Dynamic markers of altered gait rhythm in amyotrophic lateral sclerosis," *Journal of Applied Physiology*, vol. 88, no. 6, pp. 2045–2053, Jun. 2000, doi: 10.1152/jappl.2000.88.6.2045.

[9] F. Setiawan, A.-B. Liu, and C.-W. Lin, "Development of neuro-degenerative diseases' gait classification algorithm using convolutional neural network and wavelet coherence spectrogram of gait synchronization," *IEEE Access*, vol. 10, pp. 38137–38153, 2022, doi: 10.1109/ACCESS.2022.3158961.

[10] E. F. Shair, S. A. Ahmad, A. R. Abdullah, M. H. Marhaban, and S. B. M. Tamrin, "Selection of spectrogram's best window size in EMG signal during core lifting task," *Journal of Telecommunication, Electronic and Computer Engineering*, vol. 10, no. 1–16, pp. 81–85, May 2018.

[11] A. L. Goldberger *et al.*, "PhysioBank, PhysioToolkit, and PhysioNet: Components of a new research resource for complex physiologic signals," *Circulation*, vol. 101, no. 23, Jun. 2000, doi: 10.1161/01.CIR.101.23.e215.

[12] G. Shalin, S. Pardoel, J. Nantel, E. D. Lemaire, and J. Kofman, "Prediction of freezing of gait in Parkinson's disease from foot plantar-pressure arrays using a convolutional neural network," in *2020 42nd Annual International Conference of the IEEE Engineering in Medicine & Biology Society (EMBC)*, Jul. 2020, pp. 244–247, doi: 10.1109/EMBC44109.2020.9176382.

[13] R. Kumari and P. Ramachandran, "Deep CNN for Parkinson's disease classification using line spectral frequency images of sustained speech phonation," *IETE Journal of Research*, vol. 71, no. 1, pp. 341–358, Jan. 2025, doi: 10.1080/03772063.2024.2409677.

[14] K. A. Rahman, E. F. Shair, A. R. Abdullah, T. H. Lee, and N. H. Nazmi, "Deep learning classification of gait disorders in neurodegenerative diseases among older adults using ResNet-50," *International Journal of Advanced Computer Science and Applications*, vol. 15, no. 11, Nov. 2024, doi: 10.14569/IJACSA.2024.01511117.

[15] Y.-W. Ma, J.-L. Chen, Y.-J. Chen, and Y.-H. Lai, "Explainable deep learning architecture for early diagnosis of Parkinson's disease," *Soft Computing*, vol. 27, no. 5, pp. 2729–2738, Mar. 2023, doi: 10.1007/s00500-021-06170-w.

[16] W. Shao *et al.*, "A multi-modal gait analysis-based detection system of the risk of depression," *IEEE Journal of Biomedical and Health Informatics*, vol. 26, no. 10, pp. 4859–4868, Oct. 2022, doi: 10.1109/JBHI.2021.3122299.

[17] J. F. P.-Sánchez, J. M. B.-Lois, P. S.-Añó, S. M.-Casanova, and J. L.-Pascual, "Classification of Parkinson's disease stages with a two-stage deep neural network," *Frontiers in Aging Neuroscience*, vol. 15, Jun. 2023, doi: 10.3389/fnagi.2023.1152917.

[18] A. Peimankar, T. S. Winther, A. Ebrahimi, and U. K. Wiil, "A machine learning approach for walking classification in elderly people with gait disorders," *Sensors*, vol. 23, no. 2, Jan. 2023, doi: 10.3390/s23020679.

[19] E. Alushaj *et al.*, "Subregional analysis of striatum iron in Parkinson's disease and rapid eye movement sleep behaviour disorder," *NeuroImage: Clinical*, vol. 40, 2023, doi: 10.1016/j.nicl.2023.103519.

[20] D. Trabassi *et al.*, "Machine learning approach to support the detection of Parkinson's disease in IMU-based gait analysis," *Sensors*, vol. 22, no. 10, May 2022, doi: 10.3390/s22103700.

[21] S. J. Crowley *et al.*, "Statistically defined Parkinson's disease executive and memory cognitive phenotypes: demographic, behavioral, and structural neuroimaging comparisons," *Journal of Parkinson's Disease*, vol. 11, no. 1, pp. 283–297, Feb. 2021, doi: 10.3233/JPD-202166.

[22] A. Aasmann, K. K. Peper, A. Craik, and S. Haddadin, "Deep learning-based ground reaction force estimation for real-time clinical applications," *2025 47th Annual International Conference of the IEEE Engineering in Medicine and Biology Society (EMBC)*, Copenhagen, Denmark, 2025, pp. 1-6, doi: 10.1109/EMBC58623.2025.11253590.

[23] P. M. Forsman, E. M. Toppila, and E. O. Haeggstrom, "Wavelet analysis to detect gait events," *2009 Annual International Conference of the IEEE Engineering in Medicine and Biology Society*, 2009, pp. 424–427, doi: 10.1109/IEMBS.2009.5333137.

[24] F. A. Torghabeh, E. A. Moghadam, and S. A. Hosseini, "Simultaneous time-frequency analysis of gait signals of both legs in classifying neurodegenerative diseases," *Gait Posture*, vol. 113, pp. 443–451, Sep. 2024, doi: 10.1016/j.gaitpost.2024.07.302.

[25] S. Yan, Y. Cheng, Z. Hong, and P. Guoping, "The application of gait analysis in the identification, differential diagnosis and assessment of Parkinson's disease," *Chinese Journal of Neurology*, vol. 54, no. 11, pp. 1202–1207, Nov. 2021, doi: 10.3760/cma.j.cn113694-20210303-00157.

BIOGRAPHIES OF AUTHORS

Kazi Ashikur Rahman received his B.Eng. in Computer Engineering Technology (Computer Systems) in 2023 and completed his master's degree in Electrical Engineering (by research) from Universiti Teknikal Malaysia Melaka (UTeM), Malaysia. He previously gained one year of experience in software development at AppPay Sdn Bhd. He is currently a graduate research assistant at the Advanced Digital Signal Processing (ADSP) Lab, Faculty of Electrical Technology and Engineering, UTeM. His research interests include biomedical signal processing, artificial intelligence, machine learning, deep learning, and IoT. He is registered with the Board of Engineers Malaysia (BEM) and the Malaysia Board of Technologists (MBOT). He can be contacted at email: kazia096@gmail.com.

Ezreen Farina Shair received her B.Eng. in Electrical - Control and Instrumentation and M.Eng. in Electrical - Mechatronics and Automatic Control from the Universiti Teknologi Malaysia (UTM) in 2009 and 2011, respectively. Then, she received her Ph.D. in Electronics Engineering from the Universiti Putra Malaysia in 2019. Currently, she is a senior lecturer at the Universiti Teknikal Malaysia Melaka and the treasurer for the IEEE-EMBS Malaysia Chapter. She is also the technical editorial board member for the International Journal of Human and Technology Interaction (IJHaTI), and the Asian Journal of Medical Technology (AJMedTech). Her research interests are on biomedical signal processing, artificial intelligence, machine learning, deep learning, and IoT. She can be contacted at email: ezreen@utem.edu.my.

Nur Zawani Saharuddin received her diploma in Electrical Engineering and B.Eng. degree in Electrical Engineering (Industrial Power) from Universiti Teknikal Malaysia Melaka, Malaysia, in 2005 and 2008, respectively. She then received her M.Eng. degree in Electrical Engineering from University of Malaya, Malaysia, and Ph.D. degree from Universiti Tenaga Nasional, Malaysia, in 2020. Currently she serves as senior lecturer at the Faculty of Electrical Technology and Engineering, Universiti Teknikal Malaysia Melaka. Her research interests are focused on power system analysis, power system islanding, energy management, and renewable energy. She can be contacted at email: nurzawani@utem.edu.my.

Muhammad Hazwan Adlin Jumaris received his B.Sc. in Electrical Engineering in 2025 from Universiti Teknikal Malaysia Melaka (UTeM). He is currently a postgraduate student at the Advanced Digital Signal Processing (ADSP) Research Lab, Faculty of Electrical Technology and Engineering, UTeM. He is registered with the Board of Engineers Malaysia (BEM) and the Malaysia Board of Technologists (MBOT) as an engineering technologist. His research interests include biomedical signal processing, artificial intelligence, machine learning, deep learning, and IoT. He can be contacted at email: m112510012@student.utem.edu.my.